

The HLMA project: determination of high Δm^2 LMA mixing parameters and constraint on $|U_{e3}|$ with a new reactor neutrino experiment

Stefan Schönert*

Max-Planck-Institut für Kernphysik, Saupfercheckweg 1, D-69117 Heidelberg, Germany

E-mail: stefan.schoenert@mpi-hd.mpg.de

Thierry Lasserre

Max-Planck-Institut für Kernphysik, Saupfercheckweg 1, D-69117 Heidelberg, Germany

DSM/DAPNIA/SPP, CEA/Saclay, 91191 Gif-Sur-Yvette CEDEX, France

E-mail: thierry.lasserre@mpi-hd.mpg.de

Lothar Oberauer

INFN, Laboratori Nazionali del Gran Sasso, I-67010 Assergi (AQ), Italy

E-mail: lothar.oberauer@lngs.infn.it

ABSTRACT: In the forthcoming months, the KamLAND experiment will probe the parameter space of the solar large mixing angle (LMA) MSW solution as the origin of the solar neutrino deficit with $\bar{\nu}_e$'s from distant nuclear reactors. If however the solution realized in nature is such that $\Delta m_{sol}^2 \gtrsim 2 \cdot 10^{-4} \text{ eV}^2$ (thereafter named the HLMA region), KamLAND will only observe a rate suppression but no spectral distortion and hence it will not have the optimal sensitivity to measure the mixing parameters. In this case, we propose a new medium baseline reactor experiment located at Heilbronn (Germany) to pin down the precise value of the solar mixing parameters. In this paper, we present the Heilbronn detector site, we calculate the $\bar{\nu}_e$ interaction rate and the positron spectrum expected from the surrounding nuclear power plants. We also discuss the sensitivity of such an experiment to $|U_{e3}|$ in both normal and inverted neutrino mass hierarchy scenarios. We then outline the detector design, estimate background signals induced by natural radioactivity as well as by in-situ cosmic ray muon interaction, and discuss a strategy to detect the anti-neutrino signal 'free of background'.

KEYWORDS: solar and atmospheric neutrinos, reactor neutrinos, neutrino and gamma astronomy, neutrino physics, low background physics.

*Corresponding author.

Contents

1. Introduction	1
2. Experimental Site	3
3. Anti-neutrino interaction rate	4
4. Neutrino oscillation signatures	4
4.1 Two-neutrino mixing analysis	5
4.2 Three-neutrino mixing analysis	6
5. Conceptual detector design	9
6. Backgrounds	10
6.1 Non-reactor $\bar{\nu}_e$ signals	10
6.2 Backgrounds from radioactivity	11
6.2.1 External backgrounds	11
6.2.2 Internal backgrounds	12
6.3 Backgrounds induced by cosmic ray muons	13
6.3.1 Muon induced production of radioactive isotopes	14
6.3.2 Muon induced neutrons	15
7. Conclusions	15

1. Introduction

Over the last years, measurements of atmospheric and solar neutrinos gave increasing evidence for massive neutrinos and lepton mixing. Recent results of the SNO experiment combined with those of Super-Kamiokande showed for the first time directly that neutrino flavour conversion occurs [1, 2].

Whilst atmospheric neutrino measurements (dominant channel: $\nu_\mu \rightarrow \nu_\tau$) confine the oscillation parameters to $1.4 \times 10^{-3} < \Delta m_{atm}^2 < 4.2 \times 10^{-3} \text{ eV}^2$ and $\sin^2 2\Theta_{atm} > 0.9$ (90% CL) [3], solar neutrino data (dominant channel: $\nu_e \rightarrow \nu_{\mu,\tau}$) allow various disjoint areas in oscillation parameter space ranging from 10^{-10} to 10^{-3} eV^2 [4, 5, 6]. They are commonly referred to as small mixing angle (SMA), large mixing (LMA), LOW and (quasi-) vacuum (VAC) solution. The main objective of ongoing and

upcoming solar and reactor neutrino experiments is to unambiguously identify the solution and determine with high accuracy Δm_{sol}^2 and the respective mixing angle.

Solutions with $\Delta m_{sol}^2 < 10^{-6}$ eV² *or* small mixing angles can be probed best with solar neutrino experiments at sub-MeV energies [7]. Values of $\Delta m_{sol}^2 > 10^{-6}$ eV² *and* large mixing angles can be studied both with long-baseline nuclear reactor neutrino experiments [8, 9, 10] and with sub-MeV solar neutrinos [11, 12, 13]. Large mixing, in particular at large Δm_{sol}^2 values, is favoured when combining all solar neutrino data. The LMA solution gives the best χ^2 values in global analysis for $\Delta m_{sol}^2 = (3.7 - 6.3) \times 10^{-5}$ eV² and $\tan^2 \Theta_{sol} \simeq 0.35 - 0.38$ ($\sin^2 2\Theta_{sol} \simeq 0.77 - 0.80$) [4, 5, 6, 14]. Large part of the 10^{-4} eV² range is allowed by the current data. It is limited by the CHOOZ reactor experiment at $\sim 1 \times 10^{-3}$ eV² [15]. In the following we shall focus on the potential of long-baseline reactor neutrino experiments to observe neutrino oscillations and to determine Δm_{sol}^2 in case that the LMA solution is realized in nature.

Electron anti-neutrinos ($\bar{\nu}_e$) from nuclear reactors have a continuous energy spectrum up to about 10 MeV. They can be detected via inverse beta decay on protons $\bar{\nu}_e p \rightarrow e^+ n$ for $E_{\bar{\nu}_e} > E_{thr} \sim 1.8$ MeV, and their energy is derived from the measured positron kinetic energy as $E_{\bar{\nu}_e} \simeq E_{e^+} + E_{thr}$. The inverse beta decay cross section, including recoil, weak magnetism, and radiative corrections, can be found in [16].

If the distance between nuclear reactor and detector is larger than, or equal to the oscillation length, neutrino oscillations become observable as an integral reduction of the interaction rate, as well as a periodic modulation of the continuous $\bar{\nu}_e$ spectrum. For two-neutrino mixing the survival probability is

$$P_{\bar{\nu}_e \rightarrow \bar{\nu}_e} = 1 - \sin^2 2\Theta_{sol} \cdot \sin^2 \left(1.27 \frac{\Delta m_{sol}^2 [\text{eV}^2] L [\text{m}]}{E_{\bar{\nu}_e} [\text{MeV}]} \right), \quad (1.1)$$

with the mixing angle Θ_{sol} , the mass difference Δm_{sol}^2 , the reactor–detector distance L and the neutrino energy $E_{\bar{\nu}_e}$. Since the mixing angle is expected to be large, the periodic modulation of the energy spectrum should become clearly visible and the value of Δm_{sol}^2 could be derived with high accuracy.

If however, for a given value of Δm_{sol}^2 the baseline is chosen too long, adjacent peaks cannot be resolved experimentally. The shape of the positron spectrum then appears unchanged, whilst its normalization is determined by the mixing angle only, independent of the actual value of Δm_{sol}^2 . In this case only lower limits on Δm_{sol}^2 could be derived. An additional smearing can arise, if several reactors with different baseline distances contribute to the interaction rate.

Currently, there are two experiments which have the sensitivity to explore the parameter space of the solar LMA solution with $\bar{\nu}_e$'s from nuclear reactors: the neutrino signal in the KamLAND experiment in Japan is dominated by nuclear power reactors at a distance of 160 km. It is thus sensitive to probe distortions of the positron spectrum for values of $\Delta m_{sol}^2 \sim 2 \times 10^{-5}$ to $\sim 2 \times 10^{-4}$ eV² [17, 18, 19].

The BOREXINO experiment in Italy has a characteristic reactor baseline distance of about 750 km, thus would observe spectral distortions for $\Delta m_{sol}^2 \sim 4 \times 10^{-6}$ to $\sim 4 \times 10^{-5}$ eV². Both upper limits are approximate only and depend on the energy resolution that will be achieved in the experiments. A resolution of $\lesssim 10\%$ (σ) at 1 MeV is expected in KamLAND [8] and for BOREXINO an even better resolution is expected as the design goal for the light yield is about 400 pe/MeV [11].

Several authors pointed out that a dedicated reactor neutrino oscillation experiment is needed, if $\Delta m_{sol}^2 \gtrsim 2 \times 10^{-4}$ eV². The authors of Ref. [18] concluded that a baseline shorter than that of KamLAND is required in order to determine Δm_{sol}^2 in the above quoted range. The author of Ref. [7] discussed a reactor experiment with baseline of *a few 10 km* to investigate the high Δm^2 range of the LMA parameter space. First experimental details of this study were presented in [20]. The authors of Ref. [21] studied the achievable accuracy of Δm_{sol}^2 and $\tan^2\Theta$ in a hypothetical reactor experiment with a baseline of 20 km and 3000 events/year. Finally, the authors of Ref. [22] discussed the positron energy spectra for a generic reactor experiment with 20 km baseline and the accuracy of Δm_{sol}^2 determination. Moreover, the authors pointed out that for a distinct combination of mixing parameters, one can distinguish normal from inverted mass hierarchy. In summary, a new reactor neutrino experiment would become mandatory in the case that KamLAND observes a reduction of the event rate but could not resolve the characteristic oscillation pattern of the positron energy spectrum.

In this paper we propose a location and a design for a reactor neutrino experiment which would be dedicated to study, with high sensitivity, neutrino oscillations in the HLMA parameter range, i.e. $2 \times 10^{-4} \lesssim \Delta m_{sol}^2 \lesssim 10^{-3}$ eV². Moreover, we discuss a new approach to constrain $|U_{e3}|$ from the observation of “atmospheric” driven oscillation imprinted on the positron spectrum. Finally, we estimate for the proposed location and detector design, the background signals induced by natural radioactivity as well as by in-situ cosmic ray muon interaction, and discuss a strategy to detect the neutrino signal ‘free of background’.

2. Experimental Site

Requiring the first oscillation peak to appear at about 1 MeV above threshold (i.e. $E_{\bar{\nu}_e} \simeq 2.8$ MeV), the minimal distance between reactor and detector for $\Delta m_{sol}^2 = 2 \times 10^{-4}$ eV² given by Eq. (1.1) should be approximately 17 km. The detector should be located sufficiently deep underground to reduce the cosmic ray muon flux. Furthermore, the $\bar{\nu}_e$ -interaction rate should be dominated by a single baseline only to minimize the smearing of the oscillation pattern from several sources.

Various location have been investigated over the last year. Our most favoured site is a saltmine close to Heilbronn, in the south-west of Germany. More than 2000 cavernes with approximate dimensions of 15 m \times 15 m \times 150 m have been excavated

at a depth between 180 and 240 m (480 to 640 meter of water equivalent (mwe)). Two reactors are in the close, nearly equidistant vicinity: Neckarwestheim (2 cores, 6.4 GW_{th}) in southern and Obrigheim (1 core, 1.1 GW_{th}) in northern direction. Since the saltmine is extended about six kilometers in north-south direction, it is possible to select a location with a common baseline of exact 19.5 km to each of the two reactors. It is noteworthy that the Obrigheim reactor might be shut down in the very near future. In this case the baseline could be selected between 14 and 20 km, depending to which parameters the experiment needs to be optimized to. In this paper we take as generic location the position with equidistant baselines of 19.5 km to the reactors Neckarwestheim and Obrigheim.

3. Anti-neutrino interaction rate

The $\bar{\nu}_e$ spectrum above detection threshold is the result of β^- decays of $^{235,238}\text{U}$ and $^{239,241}\text{Pu}$ fission products. Measurements for ^{235}U and $^{239,241}\text{Pu}$ and theoretical calculations for ^{238}U are used to evaluate the $\bar{\nu}_e$ spectrum [23, 24]; its overall normalisation is known to about 1.4% [25] and its shape to about 2% [26]. As a nuclear reactor operates, the fission element proportions evolve in time; as an approximation we use an averaged fuel composition typical during a reactor cycle corresponding to ^{235}U (55.6 %), ^{239}Pu (32.6 %), ^{238}U (7.1 %) and ^{241}Pu (4.7 %). The mean energy release (W) per fission is then 203.87 MeV and the energy weighted cross section for $\bar{\nu}_e p \rightarrow n e^+$ amounts to $\langle \sigma \rangle_{\text{fission}} = 5.825 \times 10^{-43} \text{ cm}^2$ per fission. The reactor power (P_{th}) is related to the number of fissions per second (N_f) by $N_f = 6.241 \times 10^{18} \text{ sec}^{-1} \cdot (P_{th}[\text{MW}]) / (W[\text{MeV}])$. The event rate (R_L) at a distance L from the source, assuming no-oscillation, is then $R_L = N_f \cdot \langle \sigma \rangle_{\text{fission}} \cdot n_p \cdot 1 / (4\pi L^2)$, where n_p is the number of protons of the target. For the purpose of simple scaling, a reactor with a power of 1 GW_{th} induces a rate of 447.8 events per year in a detector with 10^{31} protons at a distance of 10 km. All relevant European nuclear plants are added in turn in order to compute the $\bar{\nu}_e$ interaction rate at the Heilbronn site. Five of them (see Tab. 1) contribute to $\sim 92\%$ of the total rate R_0 ; the other reactors contribute less than 1% to the total flux each, and 8 % in total. Assuming all reactors running at their nominal power, one expects ~ 1150 $\bar{\nu}_e$ interactions per year in a target containing 10^{31} protons (as an example, a PXE-based scintillator with a mass of 194 tons contains 10^{31} protons).

4. Neutrino oscillation signatures

A three-neutrino mixing scenario is required to explain both atmospheric and solar anomalies. In that case, flavour eigenstates $\alpha = e, \mu, \tau$ and mass eigenstates $i = 1, 2, 3$ are related through the Pontecorvo-Maki-Nakagawa-Sakata (PMNS) mixing matrix U via the relation $\nu_\alpha = \sum_{i=1}^3 U_{\alpha i} \nu_i$ [27, 28]. Assuming a “normal” mass hierarchy

Reactor	Distance [km]	Power [GW _{th}]	R_L	R_L/R_0
Neckarwestheim	19.5	6.388	754	66%
Obrigheim	19.5	1.057	125	11%
Philipsburg	54	6.842	107	9%
Biblis	80	7.420	52	4%
Grundremmingen	117	7.986	26	2%
Others (Europe)	> 100	~ 293	86	8%

Table 1: Nuclear reactor data and interaction rate at the Heilbronn site. The neutrino interaction rates R_L, R_0 are given for a target containing 10^{31} protons with the nuclear power plant running at 100% of their nominal power (typical mean values of the power vary between 80% and 90%). A PXE-based scintillator ($C_{16}H_{18}$, molar weight=210 g/mol) with a mass of 194 tons contains 10^{31} protons.

scenario, $m_1 < m_2 < m_3$, the $\bar{\nu}_e$ survival probability can be written [29, 22]

$$\begin{aligned}
P_{\bar{\nu}_e \rightarrow \bar{\nu}_e} = & 1 - 2|U_{e3}|^2(1 - |U_{e3}|^2) \left(1 - \cos \frac{\Delta m_{31}^2 L}{2E} \right) \\
& - \frac{1}{2}(1 - |U_{e3}|^2)^2 \sin^2 2\Theta_{12} \left(1 - \cos \frac{\Delta m_{21}^2 L}{2E} \right) \\
& + 2|U_{e3}|^2(1 - |U_{e3}|^2) \sin^2 \Theta_{12} \left(\cos \left(\frac{\Delta m_{31}^2 L}{2E} - \frac{\Delta m_{21}^2 L}{2E} \right) - \cos \frac{\Delta m_{31}^2 L}{2E} \right).
\end{aligned} \tag{4.1}$$

The first two terms of Eq. 4.1 contain respectively the atmospheric driven ($\Delta m_{31}^2 = \Delta m_{atm}^2$) and solar driven ($\Delta m_{21}^2 = \Delta m_{sol}^2$, $\Theta_{12} \sim \Theta_{sol}$) contributions, while the third term, absent from *any* two-neutrino mixing model, is an interference between solar and atmospheric driven oscillations. We only notice here that U_{e3} is the PMNS matrix element that couples the heaviest neutrino field to the electron field. The relative neutrino interaction rate and spectrum compared with the no-oscillation case is given, for a single reactor at a distance L from the detector, by $R/R_L = \int \Phi(E) \cdot P_{\bar{\nu}_e \rightarrow \bar{\nu}_e}(E) \cdot dE$, where Φ is the $\bar{\nu}_e$ production energy spectrum weighted by the inverse β -decay cross section. In what follows, the positron energy spectra expected from the five power plants listed in Tab. 1 are added in turn to obtain the signal at the Heilbronn site. If the KamLAND experiment points out any part of the HLMA region as the correct solution of the solar neutrino problem, the experimental signature at the Heilbronn site will be a reduction of the $\bar{\nu}_e$ rate as well as a distortion of the positron energy spectrum.

4.1 Two-neutrino mixing analysis

If $|U_{e3}|$ vanishes the lepton mixing is radically simplified and the relation 4.1 reduces then to 1.1, with $\Delta m_{21}^2 = \Delta m_{sol}^2$ and $\Theta_{12} = \Theta_{sol}$; this approximation has been used

by previous reactor neutrino experiments [15, 30]. If $|U_{e3}|^2 < 0.01$ the two-neutrino model remains valid with the small correction $\sin^2 2\Theta_{sol} = (1 - |U_{e3}|^2)^2 \sin^2 2\Theta_{12}$. The sensitivity of the experiment depends obviously on the background level that can be evaluated from the time variation of the reactor signal; at this stage, assuming no background and nuclear power plants running at their full capacity, a detector containing 10^{31} target protons would be sensitive to a 10% suppression in rate at a 3σ level after one year of data taking. Fig. 1 displays the contour lines of equal rate suppression, and thus the potential sensitivity at the Heilbronn site over the LMA region satisfying $\Delta m_{sol}^2 \gtrsim 3 \times 10^{-5} \text{ eV}^2$. In what follows, the finite energy resolution of the detector has not been included. The expected positron energy spectrum is displayed in Fig. 2 for several combinations $\Delta m_{sol}^2 - \sin^2 2\Theta_{sol}$. Since $\bar{\nu}_e$'s with different energies arrive at the Heilbronn detector with different phases, shape distortions of the positron energy spectrum are expected. These deformations depend strongly on the Δm_{sol}^2 value in the range $1 - 10 \times 10^{-4} \text{ eV}^2$; this constitutes the main advantage of a medium baseline reactor experiment over other choices, in order to measure accurately high Δm_{sol}^2 values lying in the HLMA area. The sensitivity to a distorted spectrum could extend up to a few times 10^{-3} eV^2 , depending on the achievable energy resolution. This overlaps significantly with the parameter space probed by the CHOOZ and Palo-Verde experiments [15, 30]. Whereas the precision measurement of Δm_{sol}^2 depends mainly on the energy resolution, the accuracy of the determination of the solar mixing angle will rely on the statistics as well as the control of the various backgrounds.

4.2 Three-neutrino mixing analysis

Thanks to its simplicity the two-neutrino oscillation model is a powerful tool to analyse reactor neutrino data. Nevertheless, on the baseline of interest ($\sim 20 \text{ km}$), assuming $\Delta m_{sol}^2 \lesssim \Delta m_{atm}^2$ and $U_{e3} \neq 0$, both $\bar{\nu}_e$ oscillations due to Δm_{sol}^2 (solar driven) and Δm_{atm}^2 (atmospheric driven) can develop without being averaged. This would allow to constrain the relevant $|U_{e3}|$ parameter which plays a very important role in the three-neutrino oscillation phenomenology. For instance, it drives the $\nu_\mu \leftrightarrow \nu_e$ ($\bar{\nu}_\mu \leftrightarrow \bar{\nu}_e$) oscillations of the atmospheric and (very) long baseline experiments. At present, the most stringent limit comes from the negative result from the CHOOZ experiment¹; in the case of interest $\Delta m_{sol}^2 \gtrsim 2 \cdot 10^{-4} \text{ eV}^2$, a three-neutrino mixing analysis has constrained $|U_{e3}|^2 < 0.036$ at 95 % CL, for $\Delta m_{atm}^2 = 2.5 \times 10^{-3} \text{ eV}^2$ and $\sin^2 \Theta_{sol} = 0.27$ [29]. In the forthcoming years, the long baseline accelerator experiments aim to reach a sensitivity for $|U_{e3}|^2$ down to 0.0015 (see for example [31]); a somewhat weaker constraint on $|U_{e3}|^2 = 0.003$ is expected from the K2Rdet reactor neutrino experiment [32]. On a much longer timescale, a sensitivity improved by several order of magnitude seems to be achievable with neutrino factories [33].

¹A slightly less stringent constraint has been obtained by the Palo-Verde experiment [30].

Improving our knowledge of $|U_{e3}|$ beforehand is however relevant for the design of neutrino factories. For instance, no CP-violation effect would be observable in the lepton sector if $|U_{e3}|$ vanishes or is very small. We note here that all these CP-violation effects are unambiguous in long baseline experiment only if Δm_{sol}^2 is known with a very high accuracy [18].

In that context, an additional constraint on $|U_{e3}|$ could be a by-product of the Heilbronn experiment. So as to illustrate the potential sensitivity to $|U_{e3}|$, we compute the positron spectrum obtained at the Heilbronn site with both two and three neutrino mixing scenarios, for a few $|U_{e3}| - \Delta m_{sol}^2$ combinations. For simplicity, we consider the typical set of LMA parameters $\Delta m_{sol}^2 = 5 - 80 \times 10^{-5} \text{ eV}^2$ and $\sin^2 2\Theta_{sol} = 0.8$. Taking into account the SuperKamiokande result on atmospheric neutrinos [3], we fix² $\Delta m_{atm}^2 = 2.5 \times 10^{-3} \text{ eV}^2$. The resulting spectrums are respectively displayed in Fig. 3 and Fig. 4 for $|U_{e3}|^2 = 0.04, 0.02$. The envelop of the positron spectrum is roughly given by the two-neutrino solar mixing, whereas ripples are imprinted with the “atmospheric” frequency and an amplitude proportional to $|U_{e3}|^2(1 - |U_{e3}|^2)$ (first and third term of Eq. 4.1). To detect these ripples one should be able to resolve two adjacent peaks, which are separated by $\Delta(E)$; this requires the energy resolution δE to satisfy

$$\delta E < \Delta(E) = \left(\frac{a \cdot E_{\bar{\nu}_e}^2 [\text{MeV}]}{1 - a \cdot E [\text{MeV}]} \right), \quad (4.2)$$

with $2\pi/a = 2.54 \cdot \Delta m_{atm}^2 [\text{eV}^2] \cdot L [\text{m}]$. At a baseline of 20 km, for $E_{\bar{\nu}_e} = 3, 4, 5 \text{ MeV}$, one has respectively the conditions $\delta E < 0.5, 1.0, 1.7 \text{ MeV}$. This seems to be achievable according to the energy resolution quoted by CHOOZ (0.40 MeV), and expected by KamLAND (FWHM $\sim 2.35 \times 10\% \sqrt{E} \sim 0.50 \text{ MeV}$) and BOREXINO (FWHM $\sim 2.35 \times 7\% \sqrt{E} \sim 0.35 \text{ MeV}$) over the same energy range. In addition, if one does not meet the requirement, the constraint on energy resolution could be relaxed by $\sim 25\%$ if one choses the southern site of the Heilbronn mine, located at 14 km of Neckarwestheim (which provides the bulk of the $\bar{\nu}_e$ flux).

An adequate statistics is also necessary to detect the “atmospheric” driven ripples; to obtain a *rough estimate* of the exposure needed, one can subdivide the positron energy spectrum in $\sim 0.5 \text{ MeV}$ energy bins. The statistical error has to be small enough to separate a “bump” from an adjacent “gap” (i.e 2 bins separated by an amplitude of about $4 \cdot |U_{e3}|^2(1 - |U_{e3}|^2)$), at a β sigma level. The expected bin content n_b should then satisfy $n_b \gtrsim \beta^2/16|U_{e3}|^4$. For $|U_{e3}|^2 = 0.04, 0.02, 0.01$ one obtains respectively $n_b = 40, 160, 640$ for $\beta = 1$ and $n_b = 160, 640, 2560$ for $\beta = 2$; this leads respectively to $\sim 0.9, 3.5, 14 \times 10^{31}$ and $\sim 3.5, 14, 56 \times 10^{31}$ proton-years of exposure (assuming no background, and power plants running full time at their nominal capacity). Probing $|U_{e3}|^2$ down to 0.01 corresponds to a $\sim 2\%$ relative effect

² Δm_{atm}^2 is assumed to be known at better than 10%, and slight modifications of it do not change notably the results.

on average. This is close to the systematic uncertainties on the $\bar{\nu}_e$ energy spectrum production [26], although those frequencies are expected to be lower than the “atmospheric” ripple frequencies. Finally, a complete likelihood analysis will be required to estimate accurately the detection limit of $|U_{e3}|$ as a function of Δm_{sol}^2 , exposure, and backgrounds.

For completeness, it is worthy of mention that the previous discussion remains valid if $\Delta m_{sol}^2 < 2 \times 10^{-4} \text{ eV}^2$; indeed, if $|U_{e3}|$ is not too small, whatever the Δm_{sol}^2 value measured at KamLAND, an experiment at the Heilbronn site would observe a global rate suppression from the “solar” driven neutrino oscillation and “atmospheric” ripples as discussed previously; this is illustrated in the top-left part of Fig. 3 and Fig. 4 for $\Delta m_{sol}^2 = 5 \cdot 10^{-5} \text{ eV}^2$ and $|U_{e3}|^2 = 0.04, 0.02$.

As pointed out by Petcov and Piai [22], a medium baseline reactor neutrino experiment could have the potential to distinguish between normal ($m_1 < m_2 < m_3$) and inverted ($m_3 < m_1 < m_2$) neutrino mass hierarchy. In this latter case, the heaviest neutrino field is mainly coupled to the electron neutrino field. To obtain the survival probability from Eq. 4.1 one has to apply the following permutations of indices: $2 \rightarrow 3$ and $1 \rightarrow 2$. Eq. 4.1 remains then unchanged (with now $\Delta m_{32}^2 = \Delta m_{sol}^2$ and $\Delta m_{atm}^2 = \Delta m_{31}^2$) apart from the amplitude of the interference term that can be express as $2|U_{e1}|^2(1 - |U_{e1}|^2) \cos^2 \Theta_{sol}$; notice that U_{e1} ³ is now constrained if one considers the inverted mass hierarchy model. The difference between the two hierarchies, for a medium baseline reactor neutrino experiment, is in principal observable if $\sin^2 2\Theta_{sol} \neq 1$, $|U_{e3/1}|^2 \gtrsim 0.03$, and Δm_{atm}^2 is known with a high precision [22]. At the Heilbronn site, the net difference between the two kinds of hierarchy can be seen as a shift of the phase of the “atmospheric” driven ripples on the positron energy spectrum (Fig. 4). Since the interference term has approximately the same frequency as the “atmospheric” driven oscillation term, the energy resolution requirement is also given by Eq. 4.2. The exposure needed depends mainly on the $|U_{e3/1}|$ value as discussed previously. The residuals between the two-neutrino and the three-neutrino cases normalised to the two-neutrino model $(\text{Rate}(2\nu) - \text{Rate}(3\nu)) / \text{Rate}(2\nu)$ are shown in the right part of Fig. 4, for a few Δm_{sol}^2 LMA values and $|U_{e3/1}|^2 = 0.02$. For $\Delta m_{sol}^2 < 2 \cdot 10^{-4} \text{ eV}^2$, the interference term vanishes since $\Delta m_{atm}^2 - \Delta m_{sol}^2 \sim \Delta m_{atm}^2$ and no difference can be seen between normal and inverted hierarchy. Then, Fig. 4 indicates that the difference between the two mass hierarchies could be distinguished in the narrow range $\Delta m_{sol}^2 = 2 - 4 \cdot 10^{-4} \text{ eV}^2$, while it becomes hardly detectable for higher Δm_{sol}^2 values. The ascertainable range is somewhat smaller than the one discussed in Ref. [22] with $\Delta m_{sol}^2 = 1 - 5 \cdot 10^{-4} \text{ eV}^2$. Indeed, at the Heilbronn site the interference pattern is slightly washed out since reactors at different distances are involved.

³The matrix element that couple the electron neutrino to the lightest neutrino field.

5. Conceptual detector design

At this stage, we want to line out the basic concepts of a detector design for the Heilbronn site. Detector size and energy resolution depend on the physics goals to be addressed: the determination of Δm_{sol}^2 in the HLMA parameter range can be performed with a ~ 100 ton detector, while searches for small oscillation pattern driven by the atmospheric Δm_{atm}^2 with an amplitude proportional to $|U_{e3}|^2$ requires a high event statistics, and therefore a large target mass. We estimate that $\sim 10^{32}$ proton-years are required in order to reach a sensitivity of $|U_{e3}|^2 \gtrsim 0.01$. This implies a detector similar in size to the KamLAND experiment. In order to resolve adjacent oscillation peaks, a light yield of ~ 400 pe/MeV is required for both detector sizes. A detailed analysis of the exposure (number of protons \times years) vs. sensitivity in $|U_{e3}|^2$ needs to be carried out carefully.

The detector concept proposed here is similar to that of the Counting Test Facility of BOREXINO [34], however scaled up in size and equipped with a hermetical muon veto system. It consists of concentrical spherical volumes with a liquid scintillator target at its center contained in a transparent vessel, a water buffer surrounding it, a layer of photomultiplier tubes (PMT's) viewing the scintillator target, and optically separated, an outer water buffer equipped with PMT's as a cosmic ray muon detector. A schematic view is displayed in Fig. 5.

Our current best choice for the liquid scintillator is phenyl-xylyl-ethan (PXE, $C_{16}H_{18}$) as a solvent and p-Tp and bis-MSB as fluor and secondary shifter, or alternatively PMP. PXE has a low vapor pressure ($< 1.4 \times 10^{-4}$ hPa at 20 °C) and a flash point at 149 °C, and therefore complies with general safety regulations. Moreover, the density is 0.99 g/cm³ and thus creates modest boyant forces to the scintillator containment vessel when emersed in water. Comprehensive studies of PXE based scintillators were performed in the frame of the BOREXINO project comprising optical properties, radioactive impurities and purification methods [35, 36, 37, 38]. Key results include low trace contaminations ($< 10^{-17}$ g U/g), excellent $\alpha-\beta$ discrimination, and high light yield (310 pe/MeV with 20% optical coverage).

A $\bar{\nu}_e$ event is characterized by a prompt positron event which deposits a visible energy between 1 and 8 MeV, followed by a delayed 2.2 MeV gamma event arising from neutron capture in hydrogen with $\tau \sim 200 \mu\text{sec}$. The minimal energy of 1 MeV of the prompt event is due to the positron annihilation in the scintillator. Prompt and delayed event are spatially correlated (coincidence volume $< 1 \text{ m}^3$) and both have a β/γ -type pulse shape. This characteristic signature allows to discriminate efficiently against backgrounds.

For the rest of this article, in particular for the estimation of the backgrounds, we consider the smallest useful detector size which still allows high precision determination of Δm_{sol}^2 in the HLMA parameter range. As generic dimensions we use 300 cm radius for the scintillator containment vessel, filled with a PXE based scintillator (tar-

get mass 112 ton), and an optical coverage of about 30 % providing a photo electron yield of 400/MeV. Background estimations, as discussed in the following sections, require the PMT's to be located on a sphere with a radius larger than about 500 cm. In order to shield against external radiation, an additional external water shielding of about 200 cm is necessary. This can be achieved by a cylindrical tank of about 14 m in diameter and similar in height. A schematic view of the detector layout is displayed in Fig. 5.

As a result of the background considerations we note that a detector can be realized without using a gadolinium loaded scintillator, since the accidental background rate can be suppressed to values well below one event per year. Therefore, we can achieve the highest possible light yield with liquid scintillators and hence optimize pulse shape discrimination, position reconstruction, as well as energy resolution.

6. Backgrounds

Oscillation parameters can only be determined with high accuracy if the backgrounds to reactor neutrino interaction are small. In particular, a possible observation of small $|U_{e3}|$ values depends critically on the fraction of background events which survive the acceptance cuts.

Backgrounds from primordial and man-made radioactivity can perturb neutrino detection, as well as backgrounds induced by cosmic ray interaction. Previous developments and experiments provide quantitative guidance on how to design an experiment which, in principle, allows to measure $\bar{\nu}_e$'s "free of background". In particular the Counting Test Facility of BOREXINO [39], the CHOOZ experiment [15] and measurements of muon induced production of radio-isotopes [40] provide a quantitative database as well as operational experiences.

6.1 Non-reactor $\bar{\nu}_e$ signals

Further interferences with reactor neutrinos can arise from geo-physical $\bar{\nu}_e$'s. Electron anti-neutrinos which are emitted in beta disintegration of the decay products of primordial ^{238}U and ^{232}Th in the interior of the earth have sufficient energy to create background to the reactor neutrino signal. The visible energy of the geo- $\bar{\nu}_e$ signal is below 2.4 MeV and exhibits a characteristic spectral shape. Following Ref. [41], a rate between 5 and 33 events per year and 10^{31} protons is expected at the Heilbronn site⁴. The exact value depends on the global abundance of ^{238}U and ^{232}Th in the earth's crust, mantle and core. First measurements of the geo- $\bar{\nu}_e$ flux will be performed by the KamLAND and BOREXINO experiments [41, 8, 11] and data to estimate the interference at the Heilbronn site will be available. Albeit the geo- $\bar{\nu}_e$

⁴Heilbronn is located on the continental crust. Therefore, the model developed for the interaction rate for the BOREXINO detector can be adopted.

rate is expected to be $\lesssim 3\%$ of the reactor rate, an interference with the reactor signal at low energies can not be excluded. A possibility to discard this background is to establish an analysis threshold greater than 2.4 MeV.

6.2 Backgrounds from radioactivity

Naturally occurring radioactivity can create accidental as well as correlated backgrounds. The radon daughters ^{214}Bi - ^{214}Po are a potential background of the latter type, because their decay sequence is similar to the $\bar{\nu}_e$ tag. However, the fast $\beta - \alpha$ decay with $\tau = 237 \mu\text{sec}$ can be discriminated by the energy deposition of the ^{214}Po α -decay, quenched to ~ 0.8 MeV (i.e. $> 10\sigma$ separated from the delayed 2.2 MeV γ), and in addition by pulse shape information.

Neutrons from spontaneous fission or (α, n) -reactions can produce recoil protons, subsequently thermalize and capture on hydrogen atoms. Selection of high purity materials for detector construction, passive shielding together with pulse shape discrimination provides an efficient handle against this type of correlated background. However, high energy neutrons due to cosmic ray muon interaction may contribute significantly to the background. This is discussed in detail in Sec. 6.3.2.

Gamma and beta signals in the scintillator volume may generate accidentally background events which mimic $\bar{\nu}_e$ interactions. The accidental background rate b_{acc} is given by $b_{acc} \sim b_p b_d \tau_d V_d V_{det}$. Here b_p and b_d are the specific background rates (in units of $\text{sec}^{-1} \text{m}^{-3}$) for the prompt and the delayed events, respectively. The time window for the coincidence is given by τ_d , the coincidence volume by V_d , and V_{det} is the total detection volume. In order to estimate this background rate in the detector we use the rather conservative values of $\tau_d \sim 1 \text{ msec}$ and $V_d \sim 1 \text{ m}^3$.

If the accidental background rate should be below $b_{acc} \sim 1 \text{ y}^{-1}$, and hence negligible in comparison to the neutrino interaction rate, the condition for the background rates for a $V_{det} \sim 113 \text{ m}^3$ detector then reads $b_p b_d < 3 \cdot 10^{-7} \text{ sec}^{-2} \text{m}^{-6}$. We are comparing this limit with possible contributions from different background sources.

6.2.1 External backgrounds

As external background we describe contributions due to the detector structure material (i.e. PMT's, light concentrators etc.) and the water shielding outside the liquid scintillator.

The most dangerous source for the external background is the strongly penetrating 2.6 MeV gamma line from ^{208}Tl in the Thorium chain. The typical Thorium activity reached in selected materials for all PMT's and light concentrators in the solar neutrino experiment BOREXINO is about $\sim 10^3 \text{ Bq}$ [11]. There a coverage of 30% at a distance of about 6.5m to the center of the detector is achieved. Assuming to use PMT's and light concentrators with the same specific activity at a coverage similar to BOREXINO, the background scales with the surface of the PM-sphere.

The shielding S of 2.6 MeV gammas due to the water in a spherical geometry can be parameterized by $S \sim 10^{-\alpha}$, with $\alpha \sim (R - r)/0.5m$, where R and r are the radii of the PM-sphere and the scintillator vessel, respectively.

Monte-Carlo calculations show that signals due to the external 2.6 MeV gamma line contribute with about 40 % to b_p and to about 10 % to b_d . The background rate in the total scintillator volume can be estimated to be: $b_{p-tot} \sim 10^3 \text{ sec}^{-1} \times (R/6.5m)^2 \times S$. For $R \sim 5.0m$ and $r \sim 3m$ one obtains $b_{p-tot} = 2.4 \times 10^{-2} \text{ sec}^{-1}$ and $b_{d-tot} = 6 \times 10^{-3} \text{ sec}^{-1}$. Due to the self-shielding of the scintillator these events are distributed in an outer region (roughly between 2.5m and 3m) with a total volume of about $50m^3$. Hence the specific activity at this geometry (i.e. radius of the PM-sphere at 5m) is $b_p b_d \sim 6 \cdot 10^{-8} \text{ sec}^{-2} m^{-6}$ and therefore well below the limit given above.

External backgrounds due to radioactive impurities in the water shielding have been estimated for Uranium, Thorium, and Potassium in Monte-Carlo calculations. For the prompt background all events with energies above 1 MeV have been counted. The energy window for the delayed 2.2 MeV event was chosen to be 3 sigma at a light yield of 400 photo-electrons per MeV energy deposition, corresponding to a 30% optical coverage for the PMT's and light concentrators.

The critical concentration limits obtained for Th and U in the water are in the range of about 10^{-13} g/g to 10^{-12} g/g , and for K between 10^{-10} g/g and 10^{-11} g/g , respectively. The latter obviously gives no contribution to b_d , as the 1.46 MeV gammal line from ^{40}K is far below the 2.2 MeV neutron capture energy.

For Thorium the counting rates in the total volume at a concentration of $5 \cdot 10^{-13} \text{ g/g}$ in water are $b_{p-tot} \sim 1.5 \cdot 10^{-2} \text{ sec}^{-1}$ and $b_{d-tot} \sim 3 \cdot 10^{-3} \text{ sec}^{-1}$, respectively. As these events are distributed mainly in an outer scintillator volume of about $20m^3$, the specific background therefore is $b_p b_d \sim 10^{-7} \text{ sec}^{-2} m^{-6}$ and below the allowed level given above.

For Uranium the allowed numbers are very similar and one can conclude, that for both, U and Th, a concentration lower than 10^{-12} g/g is sufficient.

These requirements for the water purity have been achieved in the Counting Test Facility (CTF) of the BOREXINO experiment [39]. Special care has to be taken for Radon in the water, which is often found to be out of the equilibrium of the U-chain. The limit given above translates to a tolerable specific Rn-activity of $\sim 10^2 \text{ mBq/m}^3$. However, also this (and even better) values have been achieved in the CTF.

6.2.2 Internal backgrounds

The acceptable single counting rates for U, Th and K within the liquid scintillator were estimated in Monte-Carlo calculations. Also here a 3 sigma window around the 2.2 MeV line for the delayed event was chosen. The results show, that the limits for concentrations of U and Th are in the level of about 10^{-13} g/g .

The results in detail: at $1 \cdot 10^{-13} \text{ g/g}$ for Uranium $b_{p-tot} \sim 1 \cdot 10^{-1} \text{ sec}^{-1}$ and $b_{d-tot} \sim 2 \cdot 10^{-2} \text{ sec}^{-1}$, are the total counting rates in the scintillator volume. As these events are distributed homogeneously all over the scintillator volume (i.e. ca. 100m^3), the specific counting rates combine to $b_p b_d \sim 2 \cdot 10^{-7} \text{ sec}^{-2} \text{ m}^{-6}$, at the design goal. A dominant part of this background comes from ^{214}Bi decay. Since the ^{214}Bi - ^{214}Po coincidence can be tagged, one can reduce the accidental background further by a about a factor 10. This translates into a a limit for the trace contamination of $< 1 \cdot 10^{-12} \text{ gU/g}$.

The same limit is basically valid for Thorium. As again the K-activity does not contribute to the delayed signal, the corresponding concentration limits are higher by about 2 orders of magnitude, i.e. in the range of about 10^{-11} g/g .

In the CTF and with neutron activation analysis of BOREXINO it has been shown [35] that even better limits have been reached with PXE as liquid solvent and p-TP as wavelengthshifter. The measured values of U and Th of the scintillator as achieved from the company was already in the 10^{-14} g/g range. After purification in a Silica-Gel column and using water extraction limits in Th and U of $2 \cdot 10^{-16} \text{ g/g}$ and $1 \cdot 10^{-17} \text{ g/g}$ have been obtained, respectively. In Tab. 2 we summarize the requirements for the principal detector components.

Source	Requirements
PMT's and concentrators	distance $\gtrsim 500 \text{ cm}$ to center
Water shield	$\lesssim 5 \times 10^{-13} \text{ g/g}$, U,Th $\lesssim 5 \times 10^{-13} \text{ g/g}$, K
Liquid Scintillator	$\lesssim 10^{-13} \text{ g/g}$, U,Th $\lesssim 10^{-11} \text{ g/g}$, K

Table 2: Summary of background requirements due to radioactive trace impurities. Trace impurities of the PMT's and light concentrators have been taken as obtained in the BOREXINO experiment [11]. The limit stated for the liquid scintillator impurities does not include the possibility to discard the ^{214}Bi - ^{214}Po coincidence on an event by event basis.

6.3 Backgrounds induced by cosmic ray muons

The rock overburden of the Heilbronn site is 180 m at ‘‘Kochendorf’’, the northern area of the Heilbronn saltmine, and 240 m at ‘‘Neubollinger Hof’’, the south western area. With a standard rock density of 2.65 g/cm^3 the depths correspond to about 480 m and 640 m of water equivalent (mwe). The underground muon fluxes, its zenith angle distribution and mean energies can be calculated following Ref. [42]. The vertical intensity at a depth of 480 (640) mwe is $9.8 (4.7) \times 10^{-6} \text{ cm}^{-2} \text{ s}^{-1} \text{ sr}^{-1}$ and the total flux, taking into account the flat surface topology, is $2.1 (1.0) \times 10^{-5} \text{ cm}^{-2} \text{ s}^{-1}$ or 760 (360)/h/m². The mean energy of the vertical flux corresponds to 72 (110) GeV.

Cosmic ray muons will be the dominating trigger rate at this depth. About six muons per second will cross a spherical scintillation target with a volume of 113 m³. The energy deposition corresponds to about 2 MeV per cm path length which provides a strong discrimination tool.

6.3.1 Muon induced production of radioactive isotopes

Long-lived muon induced isotopes can not be correlated to the primary muon interaction if their life time are much longer with respect to the characteristic time between two subsequent muon interactions. They can contribute significantly to the single trigger rate as well as simulate the $\bar{\nu}_e$ coincidence signature.

Cross sections of muon induced isotope production on liquid scintillator targets (¹²C) have been measured by the NA54 experiment at the CERN SPS muon beam at 100 GeV and 190 GeV muon energies [40]. The energy dependence was found to scale as $\sigma_{tot}(E_\mu) \propto E_\mu^\alpha$ with $\alpha = 0.73 \pm 0.10$ averaged over the various isotopes produced.

Cross sections and interaction rates are calculated for a depth of 480 mwe and summarized in Tab. 3.

	Isotopes	$T_{1/2}$	E_{max} (MeV)	$\sigma(72\text{GeV})$ (μbarn)	R_μ (sec^{-1})
β^-	¹² B	0.02 s	13.4	n.m.	-
	¹¹ Be	13.80 s	11.5	< 0.96	< 8.7×10^{-5}
	¹¹ Li	0.09 s	20.8	n.m.	
	⁹ Li	0.18 s	13.6	$1.0 \pm 0.4^*$	$(9.2 \pm 3.5) \times 10^{-5}$
	⁸ Li	0.84 s	16.0	2.3 ± 0.9	$(2.1 \pm 0.8) \times 10^{-4}$
	⁸ He	0.12 s	10.6	$1.0 \pm 0.4^*$	$(9.2 \pm 3.5) \times 10^{-5}$
	⁶ He	0.81 s	3.5	8.0 ± 1.6	$(6.9 \pm 1.7) \times 10^{-4}$
β^+, EC	¹¹ C	20.38 min	0.96	453 ± 81	$(4.0 \pm 0.8) \times 10^{-2}$
	¹⁰ C	19.30 s	1.9	61 ± 10	$(5.5 \pm 0.9) \times 10^{-3}$
	⁹ C	0.13 s	16.0	2.4 ± 1.2	$(2.1 \pm 1.1) \times 10^{-4}$
	⁸ B	0.77 s	13.7	3.3 ± 1.0	$(2.9 \pm 0.9) \times 10^{-4}$
	⁷ Be	53.3 d	0.478 (EC, γ)	100 ± 20	$(9.2 \pm 1.7) \times 10^{-3}$

Table 3: Radioactive isotopes produced by muons and their secondary shower particles in liquid scintillator targets. The rate R_μ is given for a target of 5.1×10^{30} ¹²C (with a C/H ratio of 16/18 in a pxe-based scintillator this corresponds to a 112 ton target) at a depth of 480 mwe. Because of the positron annihilation the visible energy in β^+ decays is shifted by 1.022 MeV. *: ⁹Li and ⁸He decays could not be separated experimentally. Therefore, the cross section given, corresponds to the sum of ⁹Li and ⁸He production.

The dominating background for muon induced *single* events comes from the decay of ¹¹C with a rate of about 3.5×10^3 per day or $3.6 \times 10^{-4} \text{ s}^{-1} \text{ m}^{-3}$ PXE scintillator.

It thus suffices the constraint on accidental background. *Correlated* backgrounds induced by muon interactions, can be created by β -neutron instable isotopes. Of this type of events, with ^{12}C as target, only ^8He , ^9Li and ^{11}Li are produced. The cumulative production of ^8He and ^9Li together amounts to about 3×10^3 per year for our generic target size. The characteristic signature of this class of events consists of a four-fold coincidence ($\mu \rightarrow n \rightarrow \beta \rightarrow n$). The initial muon interaction is followed by the capture of spallation neutrons within about 1 ms. The time scale of the β -decay of the considered isotopes is on the order of a few 100 ms (c.f. Tab. 3) again followed by a neutron capture. This signature allows one to discard with high efficiency this class of events maintaining a high acceptance probability for real $\bar{\nu}_e$ events.

6.3.2 Muon induced neutrons

Muon induced neutron production can be estimated from the results of the CTF experiment [39]. At LNGS the muon mean energy is 320 GeV and the flux corresponds to $1.16 \text{ m}^{-2} \text{ h}^{-1}$. Scaling the CTF production rate of $0.3 \text{ d}^{-1} \text{ t}^{-1}$ to a depth of 480 mwe, we obtain about $7.2 \times 10^3 \text{ d}^{-1}$. About a factor three higher is estimated following the compilation of Ref. [42]. A muon preceeding a neutron, therefore must not to be mistaken for a positron event with an efficiency better than one in 10^6 events.

A further source of background are neutrons which are produced in the surrounding rocks by radioactivity and in cosmic ray muon induced hadronic cascades. Neutrons can create a recoil proton and be captured by hydrogen atoms after thermalization mimicking a $\bar{\nu}_e$ event. At depths below several tens of meter, radioactive decays followed by (α, n) reactions dominate the overall flux. However, the energies involved are low and a water buffer of a modest thickness efficiently shields these neutrons. High energetic neutrons are produced in nuclear cascades up to GeV energies and above. Since the primary cosmic ray muons is not penetrating the detector, they are invisible and can not be used for discrimination purpose. High energetic neutron fluxes have been estimated for the Gran Sasso Laboratory and amount to about $25 \text{ m}^{-2} \text{ year}^{-1}$ [43]. Scaling to the depth of the Heilbronn site gives a flux of $5 \times 10^3 \text{ m}^{-2} \text{ year}^{-1}$. Assuming a surface of 113 m^2 an overall reduction factor of about 5×10^5 is required. This challenging requirement needs to be obtained by passive shielding together with active recognition of the recoil nuclei by pulse shape discrimination techniques.

7. Conclusions

In this paper we present a possible new reactor neutrino experiment with a baseline of ~ 20 km, dedicated to the accurate determination of the solar mixing parameters in the HLMA range $\Delta m_{sol}^2 \gtrsim 2 \times 10^{-4} \text{ eV}^2$. In this parameter range the KamLAND experiment would observe only a suppression of the total rate, while for the proposed

experiment the oscillations would become directly visible as an unique pattern in the positron energy spectrum. High precision determination of Δm_{sol}^2 would then become feasible. Moreover, this would provide essential input for future long baseline neutrino experiments.

We showed that an experiment at the Heilbronn site with a minimal detector mass of about 100 tons could be realized yielding an event rate of about 5×10^2 per year (in the case of no-oscillation) at a very low background rate of less than one event per year. Furthermore, we discussed that small effects related to $|U_{e3}|$ could be investigated if one increases the detector mass to about 1 kton. $|U_{e3}|^2$ could indeed be constrained down to about 0.01 and the normal and inverted neutrino mass hierarchies could be separated for a distinct combination of parameters.

Acknowledgments

S.S. would like to thank S. M. Bilenky for valuable discussions about three neutrino mixing. We are grateful to S. T. Petcov and M. Piai for discussions and for bringing to our attention Ref. [22].

References

- [1] Q. R. Ahmad *et al.* (SNO Collaboration), Phys. Rev. Lett. **87**, 071301 (2001), nucl-ex/0106015.
- [2] S. Fukuda *et al.* (Super-Kamiokande Collaboration), Phys. Rev. Lett. **86**, 5651 (2001), (hep-ex/0103032).
- [3] M. Messier (Super-Kamiokande Collaboration), NOON01 workshop, Tokyo (2001). Y. Fukuda *et al.* (Super-Kamiokande Collaboration), Phys. Rev. Lett. **81**, 1562 (1998).
- [4] J.N. Bahcall, M.C. Gonzalez-Garcia, and C. Peña-Garay, JHEP **0108**, 014 (2001), hep-ph/0106258.
- [5] G.L. Fogli, E. Lisi, D. Montanino, and A. Palazzo, Phys. Rev. **D64**, 093007 (2001), hep-ph/0106247.
- [6] M.V. Garzelli, C. Giunti, JHEP **0112**, 017 (2001), hep-ph/0108191.
- [7] S. Schönert, contribution to the proceedings of "TAUP2001 - Topics in Astroparticle and Underground Physics", LNGS, Italy (September 8-12, 2001), hep-ex/0202021.
- [8] J. Busenitz *et al.*, "Proposal for US Participation in KamLAND," March 1999 (unpublished). May be downloaded from <http://kamland.lbl.gov/>.

After completion of this paper KamLAND published first results of the detector performance (K. Inoue, First Sendai Int. Conf. on Neutrino Science, March 14-16, Sendai, Japan, <http://www.awa.tohoku.ac.jp/conf2002/program.html>). The measured energy resolution corresponds to 7.1 % (σ) at 1 MeV and is expected to improve to 5.7 % with full PMT coverage.

- [9] A. Suzuki, invited talk at 8th international workshop on neutrino telescopes, Venice, Feb. 23-26 1999.
- [10] S. Schönert, Nuclear Physics B (Proc. Suppl.) **70**, 195-198 (1999).
- [11] G. Alimonti *et al.* (BOREXINO Collaboration), Astropart. Phys. **16**, 205-234 (2002), hep-ex/0012030.
- [12] LENS Collaboration, Letter of Intent to the LNGS (1999).
- [13] Y. Suzuki *et al.*, XMASS Collaboration, NOON01, Tokyo (2000), <http://www-sk.icrr.u-tokyo.ac.jp/noon2000/index.html>.
- [14] M. Smy, contribution to the NOON01 workshop, Tokyo (2001), hep-ex/0202020.
- [15] M. Apollonio *et al.*, Phys. Lett. **B466**, 415-430 (1999), hep-ex/9907037.
- [16] P. Vogel and J. F. Beacom, Phys. Rev D **60**, 053003 (1999)
- [17] V. Barger, D. Marfatia, B. P. Wood, Phys. Lett. **B498** 53-61 (2001), hep-ph/0011251.
- [18] R. Barbieri and A. Strumia, JHEP **0012**, 016 (2000), hep-ph/0011307.
- [19] A. de Gouvêa and C. Peña-Garay, Phys. Rev. **D64**, 113011 (2001), hep-ph/0107186.
- [20] S. Schönert, Contribution to “Neutrino Oscillations and their Origin” (NOON2001), December 5-8, 2001, Tokyo, <http://www-sk.icrr.u-tokyo.ac.jp/noon2001/>, (Proc. to be published.)
- [21] A. Strumia and F. Vissani, JHEP **0111**, 048 (2001), hep-ph/0109172.
- [22] S.T. Petcov and M. Piai (2001), hep-ph/0112074.
- [23] K. Schreckenbach *et al.*, Phys. Lett. **B160**, 325 (1985).
- [24] A.A Hahn *et al.*, 1989, Phys. Lett. **B218**, 365.
- [25] Y. Declais *et al.*, Phys. Lett. **B338**, 383 (1994).
- [26] B. Achkar *et al.*, Phys. Lett. **B374**, 243 (1996).
- [27] B. Pontecorvo, Zh. Eksp. Teor. Fiz. **33**, 549 (1957), and **34**, 247 (1958).
- [28] Z. Maki, M. Nagakawa, and S. Sakata, Prog. Part. Nucl. Phys. **28**, 870 (1962).

- [29] S.M. Bilenky, D. Nicolo and S.T. Petcov (2001), hep-ph/0112216.
- [30] F. Boehm *et al.*, Phys. Rev. **D64**, 112001 (2001).
- [31] Y. Itow *et al.* (2001), hep-ex/0106019.
- [32] Y. Kozlov, L. Mikaelyan, and V. Sinev, talk presented at NANP-2001 international conference in Dubna, Russia (2001), hep-ph/0109277.
- [33] V. Barger, S. Geer, R. Raja and K. Whisnant, Phys. Rev. D **63**, 113011 (2001), hep-ph/0012017.
- [34] G. Alimonti *et al.* (BOREXINO Collaboration), Nuclear Instr. and Methods **A**, 406 411 (1998).
- [35] BOREXINO Collaboration, manuscript under preparation (2002).
- [36] R. von Hentig, PhD thesis, Physik Department E15, TU-München, (1999).
- [37] E. Resconi, PhD thesis, University of Genova (2001).
- [38] M. Göger-Neff, PhD thesis, Physik Department E15, TU-München, (2001).
- [39] G. Alimonti *et al.* (BOREXINO Collaboration), Astropart. Phys. **8**, 141 (1998).
- [40] T. Hagner, R. von Hentig, B. Heisinger, L. Oberauer, S. Schönert, F. von Feilitzsch, and E. Nolte, Astropart. Phys. **14**, 33 (2000).
- [41] R.S. Raghavan, S. Schönert, S. Enomoto, J. Shirai, F. Suekane and A. Suzuki, Phys. Rev. Lett. **80**, 635 (1998).
- [42] B.P. Heisinger, Muon-induzierte Produktion von Radionukliden, dissertation at the Physik Department E15, TU-München, (1998).
- [43] A. Dementyev *et al.*, Nucl. Phys. **B** (Proc. Suppl.), 70 486 (1999).

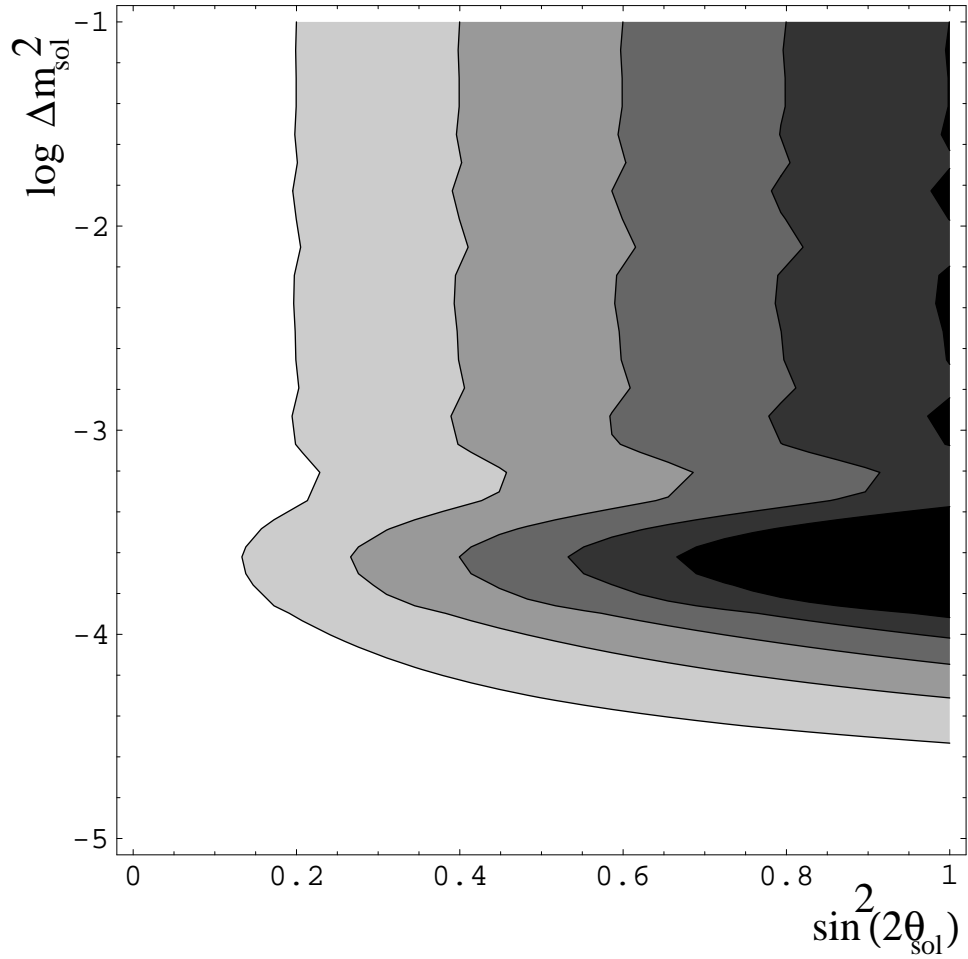


Figure 1: Contour lines of equal suppression by rates only. The first left curve represents a 10% rate suppression of the $\bar{\nu}_e$ rate, while each other line marks an additional 10% suppression step. Assuming no background, and nuclear power plants running at their full capacity, one can detect a 10% rate suppression at a 3σ level after one year of data taking with a detector containing 10^{31} target protons.

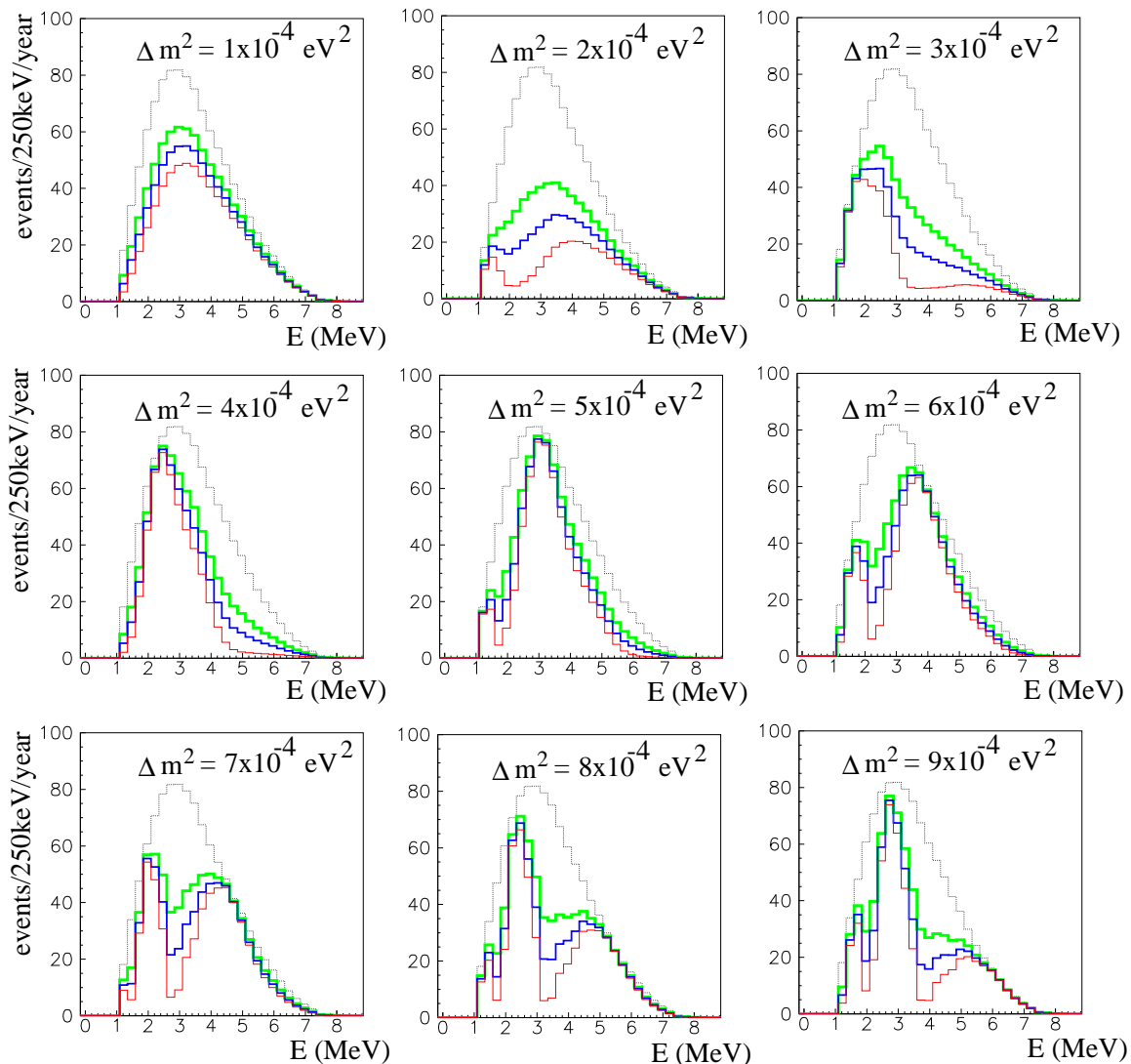


Figure 2: Positron energy spectra for various oscillation solutions assuming the power reactors to operate at their nominal power and a detector mass containing 10^{31} protons. The spectrum is binned in 250 keV intervals. The finite energy resolution has not been included. The black dotted line corresponds to the case of no oscillation. The thick light gray (green) line corresponds $\sin^2 2\Theta_{sol} = 0.6$, the medium thick black line (blue) to $\sin^2 2\Theta_{sol} = 0.8$ and the thin dark gray (red) line to $\sin^2 2\Theta_{sol} = 1.0$.

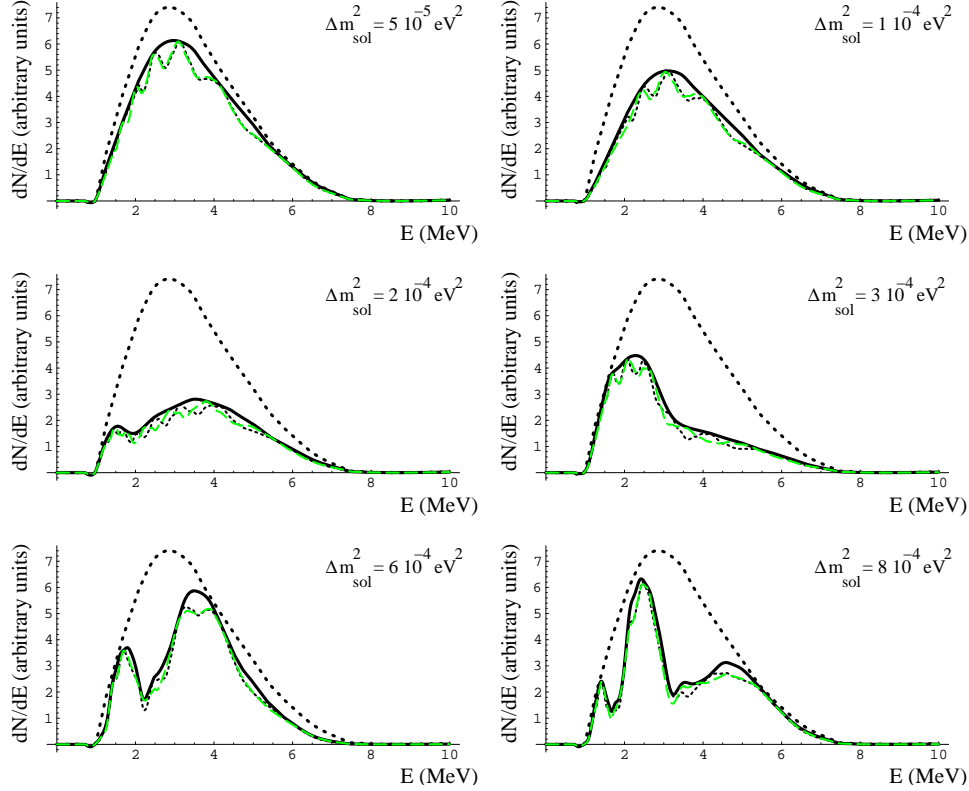


Figure 3: Difference of the positron spectrum simulated at the Heilbronn site, considering the 2ν and 3ν mixing scenarios for various oscillation solutions. The spectrums are not binned and the finite energy resolution is not included. The thick (black) dotted line corresponds to the no-oscillation case. The thick (black) line corresponds to the 2ν oscillation case (the small correction due to $|U_{e3}|$ is included in the effective mixing angle). The (black) dotted line and the thin (green) dashed line represent the 3ν oscillation case, accounting respectively for the normal and inverted hierarchy scenario. The parameter chosen are $\sin^2 2\Theta_{sol} = 0.8$, $\Delta m_{atm}^2 = 2.5 \times 10^{-3} \text{ eV}^2$, and $|U_{e3}|^2 = 0.04$ ($|U_{e1}|^2$ for the inverted hierarchy).

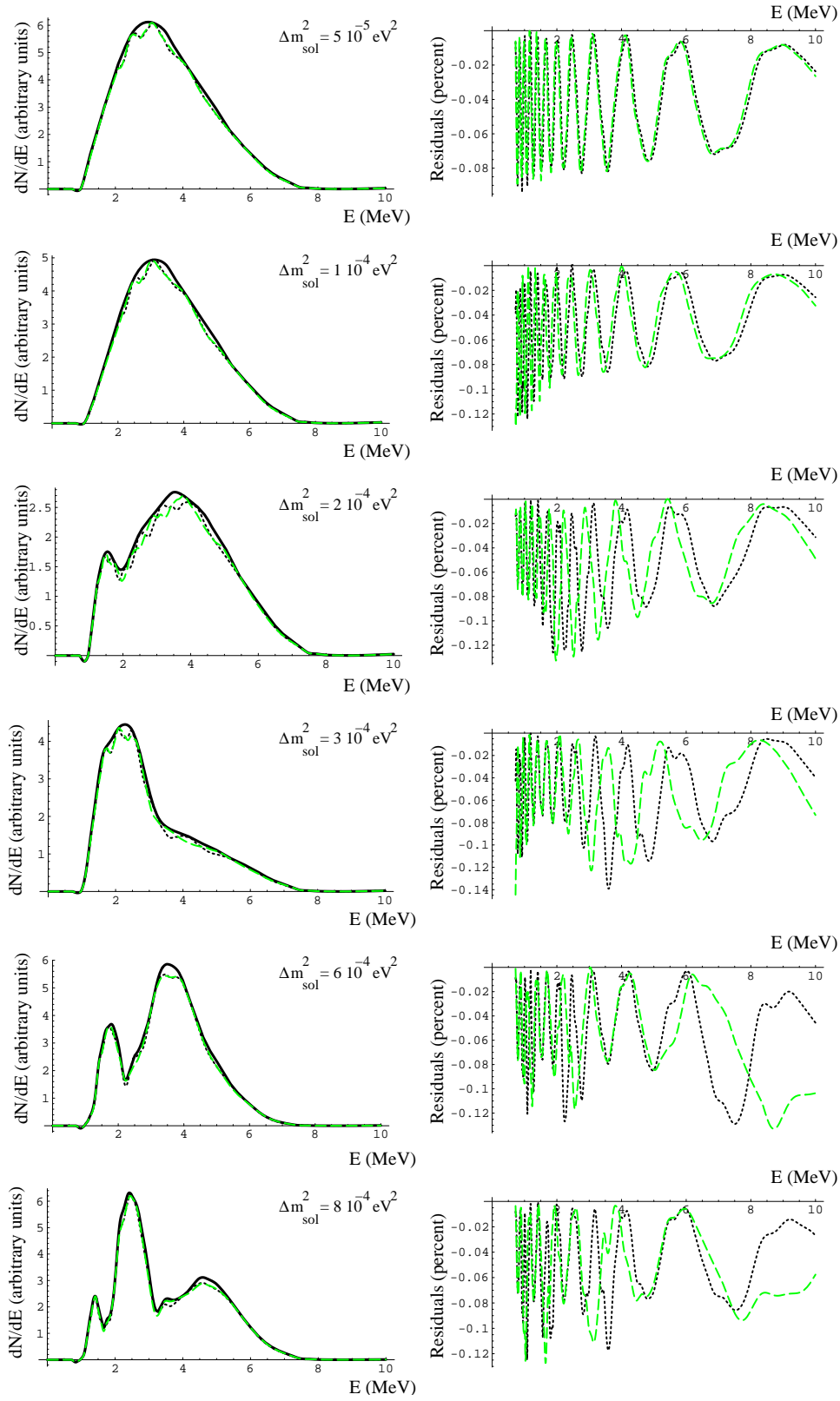


Figure 4: Three neutrino mixing positron spectrum simulated at the Heilbronn site, for various oscillation solutions (left) and corresponding residuals $(\text{Rate}(2\nu) - \text{Rate}(3\nu)) / \text{Rate}(2\nu)$ (right). The features of these graphs are the same as those of Fig. 3, except that $|U_{e3}|^2 = 0.02$ ($|U_{e1}|^2$ for the inverted hierarchy).

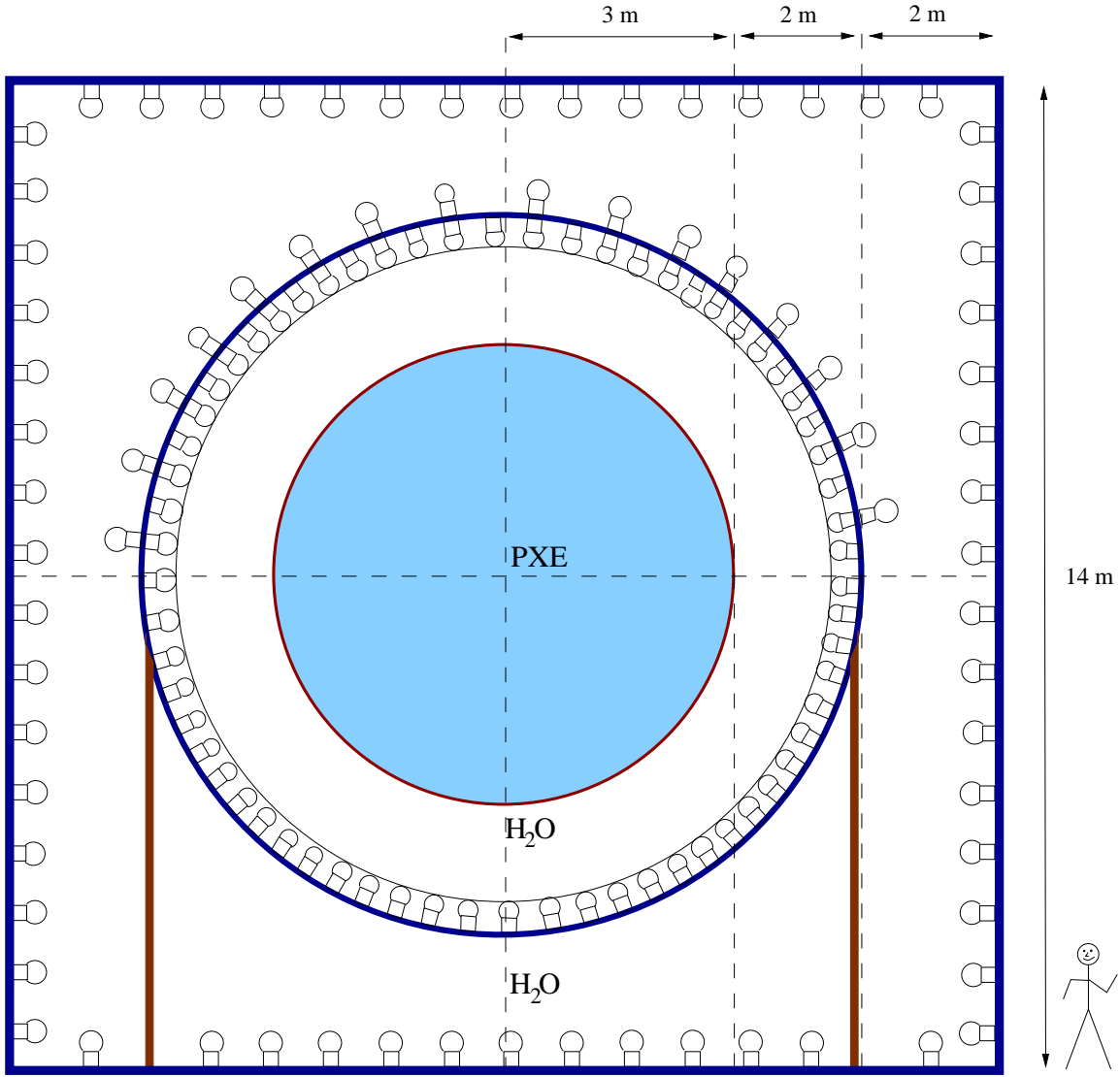


Figure 5: Schematic view of the proposed detector. Depicted is the minimal size of a detector to study the HLMA region with high accuracy at the Heilbronn underground site. About 112 tons of a PXE based liquid scintillator is contained in a transparent sphere surrounded by ultra-pure water as a passive shielding. The design goal is to achieve a light yield of about 400 pe/MeV which requires an optical coverage of about 30% provided by the surrounding PMT's and light concentrators. The PMT's are mounted on an open structure which separates optically the outer part of the detector, used as a muon veto. At this site, the depth varies between 480 and 640 mwe reducing the muon flux to about 76 to 36/h/m². The $\bar{\nu}_e$ interaction rate would be about 5×10^2 per year in the no-oscillation case. The detector design allows the background rate to be less than one event per year, provided that the design specifications of the scintillator and water buffer are met. To investigate $|U_{e3}|^2$ down to ~ 0.01 a neutrino target of about 1 kt is needed which implies to enlarge the scintillator sphere to 6.2 m radius. The tank diameter as well as height would then scale to about 20 m.